Mirror Localization for Catadioptric Imaging System by Observing Parallel Light Pairs

Ryusuke Sagawa, Nobuya Aoki, Yasushi Yagi

Institute of Scientific and Industrial Research, Osaka University,
8-1 Mihogaoka, Ibaraki-shi, Osaka, 567-0047, JAPAN
{sagawa,aoki,yagi}@am.sanken.osaka-u.ac.jp

Abstract. This paper describes a method of mirror localization to calibrate a catadioptric imaging system. While the calibration of a catadioptric system includes the estimation of various parameters, we focus on the localization of the mirror. The proposed method estimates the position of the mirror by observing pairs of parallel lights, which are projected from various directions. Although some earlier methods for calibrating catadioptric systems assume that the system is single viewpoint, which is a strong restriction on the position and shape of the mirror, our method does not restrict the position and shape of the mirror. Since the constraint used by the proposed method is that the relative angle of two parallel lights is constant with respect to the rigid transformation of the imaging system, we can omit both the translation and rotation between the camera and calibration objects from the parameters to be estimated. Therefore, the estimation of the mirror position by the proposed method is independent of the extrinsic parameters of a camera. We compute the error between the model of the mirror and the measurements, and then estimate the position of the mirror by minimizing this error. We test our method using both simulation and real experiments, and evaluate the accuracy thereof.

1 Introduction

For various applications, e.g. robot navigation, surveillance and virtual reality, a special field of view is desirable to accomplish the task. For example, omnidirectional imaging systems [1–3] are widely used in various applications. One of the main methods to obtain a special field of view, is to construct a catadioptric imaging system, which observes rays reflected by mirrors. By using various shapes of mirrors, different fields of view are easily obtained.

There are two types of catadioptric imaging systems; central and noncentral. The former has a single effective viewpoint, and the latter has multiple ones. Though central catadioptric systems have an advantage in that the image can be transformed to a perspective projection image, they have strong restrictions on the shape and position of the mirror. For example, it is necessary to use a telecentric camera and a parabolic mirror whose axis is parallel to the axis of the camera. Thus, misconfiguration can be the reason that a catadioptric system is not a central one. To obtain more flexible fields of view, several noncentral systems [4–8] have been proposed for various purposes.

For geometric analysis with catadioptric systems, it is necessary to calibrate both camera and mirror parameters. Several methods of calibration have been proposed for

central catadioptric systems. Geyer and Daniilidis [9] have used three lines to estimate the focal length, mirror center, etc. Ying and Hu [10] have used lines and spheres to calibrate the parameters. Mei and Rives [11] have used a planar marker to calibrate the parameters, which is based on the calibration of a perspective camera [12]. However, since these methods assume that the system has a single viewpoint, they cannot be applied to noncentral systems. On the other hand, several methods have also been proposed to calibrate noncentral imaging systems. Aliaga [13] has estimated the parameters of a catadioptric system with a perspective camera and a parabolic mirror using known 3D points. Strelow et al.[14] have estimated the position of a misaligned mirror using known 3D points. Micusík and Pajdla [15] have fitted an ellipse to the contour of the mirror and calibrated a noncentral camera by approximating it to a central camera. Mashita et al. [16] have used the boundary of a hyperboloidal mirror to estimate the position of a misaligned mirror. However, all of these methods are restricted to omnidirectional catadioptric systems.

There are also some approaches for calibrating more general imaging systems. Swaminathan et al. [17] computed the parameters of noncentral catadioptric systems by estimating a caustic surface from known camera motion and the point correspondences of unknown scene points. Grossberg and Nayar [18] proposed a general imaging model and computed the ray direction for each pixel using two planes. Sturm and Ramalingam [19] calibrated the camera of a general imaging model by using unknown camera motion and a known object. Since these methods estimate both the internal and external parameters of the system, the error of measurement affects the estimated result of all of the parameters.

In this paper, we focus on the localization of the mirror in the calibration of catadioptric systems. Assumptions of the other parameters are as follows:

- The intrinsic parameters, such as the focal length and principal point of a camera, are known.
- The shape of the mirror is known.

The only remaining parameters to be estimated are the translation and rotation of the mirror with respect to the camera. If we calibrate the parameters of an imaging system by observing some markers, it is necessary to estimate the extrinsic parameters, such as rotation and translation, with respect to the marker. If we include these parameters as parameters to be estimated, the calibration results are affected by them. We proposed a method to localize a mirror by observing a parallel light [20] that estimates the mirror parameters independently of the extrinsic parameters. Since the translation between a marker and a camera is omitted from the estimation, this method can reduce the number of parameters. The method however, needs a rotation table to observe a parallel light from various directions. Instead of using a rotation table, the method proposed in this paper observes pairs of parallel lights as calibration markers. We can therefore, omit both rotation and translation from the estimation and reduce the number of parameters that are affected by the measurement error in the calibration.

We describe the geometry of projection of two parallel lights in Section 2. Next, we propose an algorithm for mirror localization using pairs of parallel lights in Section 3. We test our method in Section 4 and finally summarize this paper in Section 5.

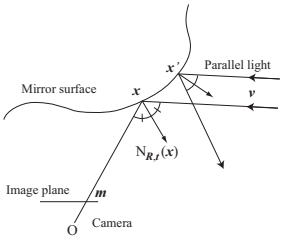

Fig. 1. Projecting a parallel light onto a catadioptric imaging system.

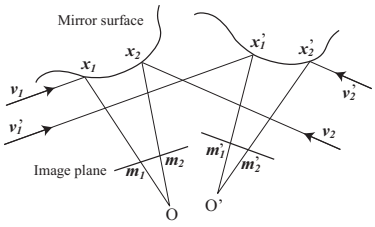

Fig. 2. Projecting a pair of parallel lights with two different camera positions and orientations.

2 Projecting a Pair of Parallel Lights onto a Catadioptric Imaging System

In this section, we first explain the projection of a parallel light, which depends only on the rotation of a camera. Next, we describe the projection of a pair of parallel lights and the constraint on the relative angle between them.

2.1 Projecting a Parallel Light

First, we explain the projection of a parallel light. Figure 1 shows the projection of a parallel light onto a catadioptric system. Since a parallel light is not a single ray, but a bunch of parallel rays, such as sunlight, it illuminates the whole catadioptric system. $\boldsymbol{v}$ is the vector of the incident parallel light. $\boldsymbol{m}$ is the vector at the point onto which the light is projected. $\boldsymbol{m}$ is computed as follows:

$$\boldsymbol{m} = K^{-1}\hat{\boldsymbol{p}}, \tag{1}$$

where $\hat{\boldsymbol{p}} = (p_x, p_y, 1)$ is the point onto which the light is projected in the homogeneous image coordinate system. K is a 3×3 matrix that represents the intrinsic parameters of the camera. Although the incident light is reflected at every point on the mirror surface where the mirror is illuminated, the reflected light must go through the origin of the camera to be observed. Since the angle of the incident light is the same as that of the reflected light, the camera only observes the ray reflected at a point $\boldsymbol{x}$. Therefore, the equation of projection becomes

$$-\boldsymbol{v} = \frac{\boldsymbol{m}}{\parallel \boldsymbol{m} \parallel} + 2(N_{R,\boldsymbol{t}}(\boldsymbol{x}) \cdot \frac{\boldsymbol{m}}{\parallel \boldsymbol{m} \parallel})N_{R,\boldsymbol{t}}(\boldsymbol{x}), \tag{2}$$

where $N_{R,\boldsymbol{t}}(\boldsymbol{x})$ is the normal vector of the mirror surface at the point $\boldsymbol{x}$. R and $\boldsymbol{t}$ are the rotation and translation, respectively, of the mirror relative to the camera.

2.2 Projecting a Pair of Parallel Lights

Since the direction of the incident parallel light is invariant even if it is observed from different camera positions, the direction of the light relative to the camera depends only

on the orientation of the camera. Now, if we observe two parallel lights simultaneously, the relative angle between these parallel lights does not change irrespective of the camera orientation. Figure 2 shows a situation, in which a pair of parallel lights is projected onto a catadioptric system, and which has two different camera positions and orientations. The relative position of the mirror is fixed to the camera. The two parallel lights are reflected at the points $\boldsymbol{x}_1$, $\boldsymbol{x}_2$, $\boldsymbol{x}'_2$ and $\boldsymbol{x}'_1$, respectively. The reflected rays are projected onto the points $\boldsymbol{m}_1$, $\boldsymbol{m}_2$, $\boldsymbol{m}'_2$ and $\boldsymbol{m}'_1$ in the image plane, respectively.

Since the relative angle between the pair of parallel lights is invariant, we obtain the following constraint:

$$\boldsymbol{v}_1 \cdot \boldsymbol{v}_2 = \boldsymbol{v}'_1 \cdot \boldsymbol{v}'_2, \tag{3}$$

where $\boldsymbol{v}'_1$ and $\boldsymbol{v}'_2$ are represented in a different camera coordinate system from $\boldsymbol{v}_1$ and $\boldsymbol{v}_2$, which are computed by (2).

3 Mirror Localization using Pairs of Parallel Lights

This section describes an algorithm to estimate mirror position by observing pairs of parallel lights.

3.1 Estimating Mirror Position by Minimizing Relative Angle Error

By using the constraint (3), we estimate the mirror position by minimizing the following cost function:

$$E_1 = \sum_i \parallel \boldsymbol{v}_{i1} \cdot \boldsymbol{v}_{i2} - \cos\alpha_i \parallel^2, \tag{4}$$

where i is the number of the pair and α_i is the angle of the i-th pair. If we do not know the angle between the parallel lights, we can use

$$E_2 = \sum_{i \neq j} \parallel \boldsymbol{v}_{i1} \cdot \boldsymbol{v}_{i2} - \boldsymbol{v}_{j1} \cdot \boldsymbol{v}_{j1} \parallel^2 . \tag{5}$$

The parameters of these cost functions are R and $\boldsymbol{t}$, which are the rotation and translation, respectively, of the mirror relative to the camera. Since minimizing (4) or (5) is a nonlinear minimization problem, we estimate R, $\boldsymbol{t}$ and R_C by a nonlinear minimization method, such as the Levenberg-Marquardt algorithm. Our algorithm can then be described as follows:

1. Set initial parameters of R and $\boldsymbol{t}$.
2. Compute the intersecting point $\boldsymbol{x}$ for each image point $\boldsymbol{m}$.
3. Compute the normal vector $N_{R,\boldsymbol{t}}(\boldsymbol{x})$ for each intersecting point $\boldsymbol{x}$.
4. Compute the incident vector $\boldsymbol{v}$ for each intersecting point $\boldsymbol{x}$.
5. Compute the cost function (4) or (5).
6. Update R and $\boldsymbol{t}$ by a nonlinear minimization method.
7. Repeat steps 2-6 until convergence.

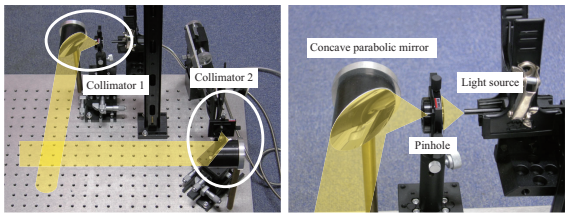

Fig. 3. Two collimators generate a pair of parallel lights. Each collimator consists of a light source, a pinhole and a concave parabolic mirror.

In the current implementation, the initial parameters are given by user. We set them so that the every image point $\boldsymbol{m}$ has the intersecting point $\boldsymbol{x}$. As described in Section 3.2, computing the intersecting points is high cost if a mirror surface is represented by a mesh model. Therefore, we describe a GPU-based method for steps 2-4 to directly compute the incident vectors to reduce the computational time. For updating the parameters, we numerically compute the derivatives required in the Levenberg-Marquardt algorithm. To keep so that every image point has the intersecting point, if an image point has no intersecting point, we penalize it with a large value instead of computing (4) or (5).

3.2 Computing the Incident Vector

The important step in this algorithm is the computation of the incident vector $\boldsymbol{v}$, for which there are two methods. The first of these computes $\boldsymbol{x}$ by solving a system of equations. If the mirror surface is represented as a parametric surface, $\boldsymbol{x}$ is obtained by simultaneously solving the equations of the viewing ray and the mirror surface, because the intersecting point $\boldsymbol{x}$ is on both the viewing ray and the mirror surface. Once $\boldsymbol{x}$ is computed, the normal vector $N_{R,\boldsymbol{t}}(\boldsymbol{x})$ is obtained by the cross product of two tangential vectors of the mirror surface at $\boldsymbol{x}$, and then the incident vector $\boldsymbol{v}$ is computed by (2).

However, it is high cost to solve the simultaneous equations if the mirror surface is an intricate shape or non-parametric surface. If a mirror surface is represented as a mesh model, it is necessary to search the intersecting point for each image point by solving the equations for each facet of the model. To accommodate any mirror shape, the second method computes $\boldsymbol{x}$ by projecting the mirror shape onto the image plane of the camera with R, $\boldsymbol{t}$ and the intrinsic parameter K. Since this operation is equivalent to rendering the mirror shape onto the image plane, it can be executed easily using computer graphics techniques if the mirror shape is approximated by a mesh model. Furthermore, if we use recent graphics techniques, the incident vector $\boldsymbol{v}$ is computed directly by the rendering process. The source code to compute $\boldsymbol{v}$ for every pixel is shown in Appendix A.

3.3 Generating a Pair of Parallel Lights

Our proposed method requires observation of parallel lights. A parallel light can be viewed by adopting one of the following two approaches:

– Use a feature point of a distant marker.
– Generate a collimated light.

In the former approach, a small translation of camera motion can be ignored because it is much smaller than the distance to the marker. Thus, the ray vector from the feature point is invariant even if the camera moves. The issue of this approach is a lens focus problem. When the focus setting of the camera is not at infinite focus, the image is obtained with a minimum aperture and long shutter time to avoid a blurred image. Instead of using distant points to obtain two parallel lights, vanishing points can be used. Some methods [21–23] was proposed for the calibration of a perspective camera.

In the latter approach, a parallel light is generated by a collimator. A simple method is to use a concave parabolic mirror and a point-light source. Figure 3 shows an example of such a system. By placing pinholes in front of the light sources, they become point-light sources. Since pinholes are placed at the focus of the parabolic mirrors, the reflected rays are parallel. The illuminated area is indicated in yellow in the figure. The advantage of this approach is that a small and precise system can be constructed although optical apparatus is required.

4 Experiments

4.1 Estimating Accuracy by Simulation

We first evaluate the accuracy of our method by simulation. In this simulation, we estimate the position of a parabolic mirror relative to a perspective camera. The intrinsic parameter K of the perspective camera is represented as

$$K = \begin{pmatrix} f & 0 & c_x \\ 0 & f & c_y \\ 0 & 0 & 1 \end{pmatrix}. \tag{6}$$

The shape of the mirror is represented as $z = \frac{1}{2h}(x^2 + y^2)$, where h is the radius of a paraboloid. In this experiment, the image size is 512×512 pixels and $f = 900$, $c_x = c_y = 255$ and $h = 9.0$. The ground truths of the rotation and translation of the mirror are $R = I$ and $\boldsymbol{t} = (0, 0, 50)$, respectively. We tested two relative angles between two incident parallel lights, namely 30 and 90 degrees. 24 pairs of the incident lights are used by rotating the camera and mirror around the y- and z-axes.

We estimate R and $\boldsymbol{t}$ by adding noise to the position of the input points. The added Gaussian noise has standard deviations of 0, 0.1, 0.5, and 1.0 pixels. As for E_1, since the relative angle α between the two points has to be given, we add noise to α, which has standard deviations of 0, 0.1, and 0.5 degrees. To evaluate the accuracy of the estimated parameters, we compute the root-mean-square (RMS) errors between the input points and the reprojection of the incident lights. Figure 4 shows the RMS errors of E_1 and E_2. It is clear that the results obtained with the relative angle equal to 90 degrees are better than those for 30 degrees. A reason for this may be that the constraint is weaker when the relative angle is smaller and the projected points are close to each other. The error depends mainly on the noise of the input points, as the effect of the noise of the

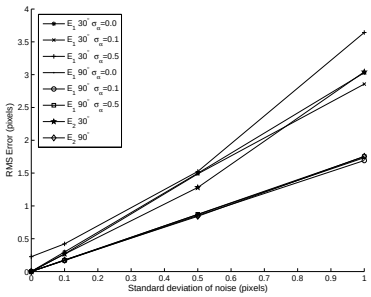

Fig. 4. The RMS errors with respect to the noise of image points.

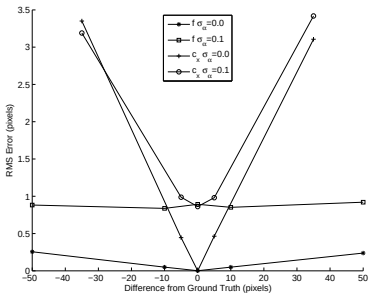

Fig. 5. The RMS errors with respect to the error of the intrinsic parameters.

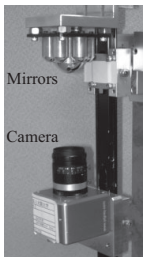

Fig. 6. Compound parabolic mirrors attached to a camera.

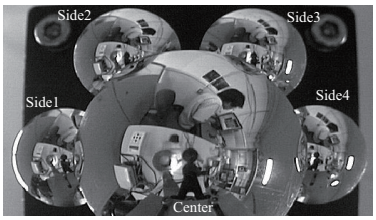

Fig. 7. An example image from compound parabolic mirrors.

relative angle is small. Since the accuracy of E_2 is similar to that of E_1, we can apply our method even if we do not know the relative angle.

Next, we evaluate the error if the intrinsic parameter K is different from the ground truth. Figure 5 shows the RMS errors of E_1 with varying values of f and c_x. The other parameters are fixed to the ground truth. The horizontal axis means the difference between the ground truth and f or c_x. The results show that the error from reprojecting the incident lights is significantly affected by c_x, while the effect of f is small. This shows that the principal point (c_x, c_y) must be computed accurately before minimizing E_1 and that the error of f is more acceptable than that of the principal point.

4.2 Localizing Mirrors from Real Images

In the next experiment, we compute the mirror positions of a catadioptric system with compound parabolic mirrors [24, 25] as shown in Figure 6. Figure 7 shows an example of an image obtained from such a system. Our system has 7 parabolic mirrors and a perspective camera, PointGrey Scorpion, which has 1600×1200 pixels and about 22.6° field of view. The distortion of the lens is calibrated by the method described in [26], and the intrinsic parameters of the camera are already calibrated. With this setup, the catadioptric system is not single viewpoint. The radii h of a center mirror and the side mirrors are 9.0mm and 4.5mm, respectively. The diameter and height of the

Fig. 8. A distant point used as a parallel light source.

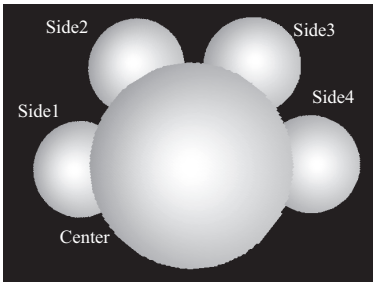

Fig. 9. The mirror positions estimated by the proposed method.

center mirror are 25.76mm and 9.0mm, respectively, and the diameter and height of the side mirrors are 13.0mm and 4.5mm, respectively. The diameters of the center and side mirrors projected onto the image are 840 and 450 pixels, respectively.

To localize the mirrors from real images, we experimented with different ways of acquiring parallel lights, namely distant markers and collimated lights.

In the first case, we chose points on a distant object in the image. Figure 8 shows the chosen point, which is a point on a building that is about 260 meters away from the camera. We rotated the catadioptric system and obtained 78 pairs of parallel lights. The relative angles of the pairs of parallel lights vary between 15 degrees and 170 degrees. We estimated the positions of the center and four side mirrors independently. Figure 9 shows the estimated mirror positions by rendering the mirror shapes from the viewpoint of the camera. Since we do not know the ground truth of the mirror position and the incident light vectors, we estimate the accuracy of the estimated parameters by the following criterion. If the observed points of a pair of parallel lights are $\boldsymbol{p}_1$ and $\boldsymbol{p}_2$, and the corresponding incident vectors, as computed by (2), are $\boldsymbol{v}_1$ and $\boldsymbol{v}_2$, respectively,

$$\min_{\boldsymbol{q}} \sqrt{\| \boldsymbol{p}_2 - \boldsymbol{q} \|^2} \quad \text{subject to} \quad \boldsymbol{v_q} \cdot \boldsymbol{v}_1 = \cos\alpha, \tag{7}$$

where $\boldsymbol{v_q}$ is the incident vector corresponding to an image point $\boldsymbol{q}$. This criterion computes the errors in pixels. Table 1 shows the estimated results. Since some of the lights are occluded by the other mirrors, the number of lights used for calibration varies for each mirror. The error is computed by the RMS of (7). Since the position of a feature point is considered to have 0.5 pixel error, the error computed by using the estimated position of the mirrors is appropriate.

Next, we tested our method by observing collimated lights generated by the system shown in Figure 3. The relative angle of the two collimated lights is 87.97 degrees. We acquired 60 pairs of parallel lights. Figure 10 shows an example of an image, onto which two collimated lights are projected. In this experiment, we estimated the position of the center mirror. The RMS error of (7) is 0.35 pixels, which is smaller than that obtained using distant markers. This shows that the accuracy of the estimated results is improved by using the collimated lights.

Table 1. The RMS errors of (7) are computed using the estimated mirror positions.

Mirror	Number of Pairs	RMS Error (pixels)
Center	78	0.84
Side1	21	0.87
Side2	45	1.05
Side3	45	1.16
Side4	21	0.59

5 Conclusion

This paper describes a method of mirror localization to calibrate a catadioptric imaging system. In it, we focused on the localization of the mirror. By observing pairs of parallel lights, our method utilizes the constraint that the relative angle of two parallel lights is invariant with respect to the translation and rotation of the imaging system. Since the translation and rotation between a camera and the calibration objects are omitted from the parameters, the only parameter to be estimated is the rigid transformation of the mirror. Our method estimates the rigid transformation by minimizing the error between the model of the mirror and the measurements. Since our method makes no assumptions about the mirror shape or its position, the proposed method can be applied to noncentral systems. If we compute the incident light vector by projecting the mirror shape onto an image, our method is able to accommodate any mirror shape. Finally, to validate the accuracy of our method, we tested our method in a simulation and in real experiments. For future work, we plan to apply the proposed method to various shapes of mirrors using the collimated lights and analyzing the best settings for the parallel lights.

A Source Code for Rendering Incident Vectors

The reflected vector for each pixel is computed using the source code in Figure 11. It is written in High-Level Shader Language (HLSL) and executed by graphics hardware. The shape of a mirror is represented by a mesh model that consists of vertices and triangles. The inputs of the vertex shader (`VS`) are the positions of vertices of the mirror (`Pos`) and the normal vectors of the vertices (`Nor`). `R`, `T` and `KT` are constant matrices given by a main program. `R` is the rotation matrix of the mirror, and `T` = $[R|\boldsymbol{t}]$, where $\boldsymbol{t}$ is the translation vector of the mirror. `KT` is the projection matrix computed as `KT` = $K[R|\boldsymbol{t}]$, where K is the intrinsic matrix of the camera. The reflected vector `v` is computed for each vertex. Since it is interpolated by the rasterizer of the graphics hardware, the pixel shader (`PS`) outputs the reflected vector for each pixel.

References

1. Ishiguro, H., Yamamoto, M., Tsuji, S.: Omni-directional stereo. IEEE Transactions on Pattern Analysis and Machine Intelligence **14**(2) (1992) 257–262

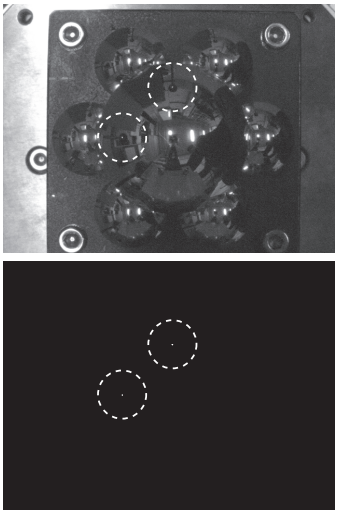

Fig. 10. Top: an example of the acquired image. Bottom: the image of two collimated lights after turning off the room light.

```
struct VS_OUT {
  float4 Pos  : POSITION;
  float3 Tex : TEXCOORD0;
};
VS_OUT VS(float4 Pos : POSITION,
          float4 Nor : NORMAL)
{
  VS_OUT Out = (VS_OUT)0;
  float3 tmpPos, tmpNor, v;
  float a;
  tmpPos = normalize(mul(Pos, T));
  tmpNor = mul(Nor, R);
  a = dot(-tmpPos, tmpNor);
  v = tmpPos + 2 * a * tmpNor;
  Out.Pos = mul(Pos, KT);
  Out.Tex = normalize(v);
  return Out;
}
float4 PS(VS_OUT In) : COLOR
{
  float4 Col = 0;
  Col.rgb = In.Tex.xyz;
  return Col;
}
```

Fig. 11. The source code for computing the incident vector in HLSL.

2. Yamazawa, K., Yagi, Y., Yachida, M.: Obstacle detection with omnidirectional image sensor hyperomni vision. In: IEEE the International Conference on Robotics and Automation, Nagoya (1995) 1062 – 1067
3. Nayar, S.: Catadioptric omnidirectional camera. In: Proc. IEEE Computer Society Conference on Computer Vision and Pattern Recognition. (1997) 482–488
4. Gaspar, J., Decco, C., Jr., J.O., Santos-Victor, J.: Constant resolution omnidirectional cameras. In: Proc. the Third Workshop on Omnidirectional Vision. (2002) 27–34
5. Hicks, R., Perline, R.: Equi-areal catadioptric sensors. In: Proc. the Third Workshop on Omnidirectional Vision. (2002) 13–18
6. Swaminathan, R., Nayar, S., Grossberg, M.: Designing Mirrors for Catadioptric Systems that Minimize Image Errors. In: Fifth Workshop on Omnidirectional Vision. (2004)
7. Kondo, K., Yagi, Y., Yachida, M.: Non-isotropic omnidirectional imaging system for an autonomous mobile robot. In: Proc. 2005 IEEE International Conference on Robotics and Automation, Barcelona, Spain (2005)
8. Kojima, Y., Sagawa, R., Echigo, T., Yagi, Y.: Calibration and performance evaluation of omnidirectional sensor with compound spherical mirrors. In: Proc. The 6th Workshop on Omnidirectional Vision, Camera Networks and Non-classical cameras. (2005)
9. Geyer, C., Daniilidis, K.: Paracatadioptric camera calibration. IEEE Transactions on Pattern Analysis and Machine Intelligence **24**(5) (2002) 687–695
10. Ying, X., Hu, Z.: Catadioptric camera calibration using geometric invariants. IEEE Transactions on Pattern Analysis and Machine Intelligence **26**(10) (2004) 1260–1271
11. Mei, C., Rives, P.: Single view point omnidirectional camera calibration from planar grids. In: Proc. 2007 IEEE International Conference on Robotics and Automation, Rome, Italy (2007) 3945–3950
12. Hartley, R.I., Zisserman, A.: Multiple View Geometry in Computer Vision. Second edn. Cambridge University Press, ISBN: 0521540518 (2004)

13. Aliaga, D.: Accurate catadioptric calibration for realtime pose estimation of room-size environments. In: Proc. IEEE International Conference on Computer Vision. Volume 1. (2001) 127–134
14. Strelow, D., Mishler, J., Koes, D., Singh, S.: Precise omnidirectional camera calibration. In: Proc. of IEEE Conference on Computer Vision and Pattern Recognition. Volume 1. (2001) 689–694
15. Micusík, B., Pajdla, T.: Autocalibration and 3d reconstruction with non-central catadioptric cameras. In: Proc. IEEE Computer Society Conference on Computer Vision and Pattern Recognition. Volume 1., Washington US (2004) 58–65
16. Mashita, T., Iwai, Y., Yachida, M.: Calibration method for misaligned catadioptric camera. In: Proc. the Sixth Workshop on Omnidirectional Vision. (2005)
17. Swaminathan, R., Grossberg, M., Nayar, S.: Caustics of catadioptric camera. In: Proc. IEEE International Conference on Computer Vision. Volume 2. (2001) 2–9
18. Grossberg, M., Nayar, S.: The raxel imaging model and ray-based calibration. International Journal on Computer Vision **61**(2) (2005) 119–137
19. Sturm, P., Ramalingam, S.: A generic camera calibration concept. In: Proc. European Conference on Computer Vision. Volume 2., Prague, Czech (2004) 1–13
20. Sagawa, R., Aoki, N., Mukaigawa, Y., Echigo, T., Yagi, Y.: Mirror localization for a catadioptric imaging system by projecting parallel lights. In: Proc. IEEE International Conference on Robotics and Automation, Rome, Italy (2007) 3957–3962
21. Caprile, B., Torre, V.: Using vanishing points for camera calibration. International Journal of Computer Vision **4**(2) (1990) 127–140
22. Daniilidis, K., Ernst, J.: Active intrinsic calibration using vanishing points. Pattern Recognition Letters **17**(11) (1996) 1179–1189
23. Guillemaut, J., Aguado, A., Illingworth, J.: Using points at infinity for parameter decoupling in camera calibration. IEEE Transactions on Pattern Analysis and Machine Intelligence **27**(2) (2005) 265–270
24. Mouaddib, E., Sagawa, R., Echigo, T., Yagi, Y.: Two or more mirrors for the omnidirectional stereovision? In: Proc. of The second IEEE-EURASIP International Symposium on Control, Communications, and Signal Processing, Marrakech, Morocco (2006)
25. Sagawa, R., Kurita, N., Echigo, T., Yagi, Y.: Compound catadioptric stereo sensor for omnidirectional object detection. In: Proc. IEEE/RSJ International Conference on Intelligent Robots and Systems. Volume 2., Sendai, Japan (2004) 2612–2617
26. Sagawa, R., Takatsuji, M., Echigo, T., Yagi, Y.: Calibration of lens distortion by structured-light scanning. In: Proc. 2005 IEEE/RSJ International Conference on Intelligent Robots and Systems, Edmonton, Canada (2005) 1349–1354